Title

Activation Mechanisms of Conventional Protein Kinase C Isoforms Are Determined by the Ligand Affinity and Conformational Flexibility of Their C1 Domains*

Journal

Journal of Biological Chemistry, 278(47)

ISSN

0021-9258

Authors

Ananthanarayanan, Bharath
Stahelin, Robert V
Digman, Michelle A
et al.

Publication Date

2003-11-01

DOI

10.1074/jbc.m307853200

THE JOURNAL OF BIOLOGICAL CHEMISTRY
Vol. 278, No. 47, Issue of November 21, pp. 46886–46894, 2003

Printed in U.S.A.

Activation Mechanisms of Conventional Protein Kinase C Isoforms Are Determined by the Ligand Affinity and Conformational Flexibility of Their C1 Domains*

Received for publication, July 21, 2003, and in revised form, August 28, 2003
Published, JBC Papers in Press, September 3, 2003, DOI 10.1074/jbc.M307853200

Bharath Ananthanarayanan, Robert V. Stahelin, Michelle A. Digman, and Wonhwa Cho‡

From the Department of Chemistry, University of Illinois at Chicago, Chicago, Illinois 60607

The regulatory domains of conventional and novel protein kinases C (PKC) have two C1 domains (C1A and C1B) that have been identified as the interaction site for diacylglycerol (DAG) and phorbol ester. It has been reported that C1A and C1B domains of individual PKC isoforms play different roles in their membrane binding and activation; however, DAG affinity of individual C1 domains has not been quantitatively determined. In this study, we measured the affinity of isolated C1A and C1B domains of two conventional PKCs, PKCα and PKCγ, for soluble and membrane-incorporated DAG and phorbol ester by isothermal calorimetry and surface plasmon resonance. The C1A and C1B domains of PKCα have opposite affinities for DAG and phorbol ester; *i.e.* the C1A domain with high affinity for DAG and the C1B domain with high affinity for phorbol ester. In contrast, the C1A and C1b domains of PKCγ have comparably high affinities for both DAG and phorbol ester. Consistent with these results, mutational studies of full-length proteins showed that the C1A domain is critical for the DAG-induced activation of PKCα, whereas both C1A and C1B domains are involved in the DAG-induced activation of PKCγ. Further mutational studies in conjunction with *in vitro* activity assay and monolayer penetration analysis indicated that, unlike the C1A domain of PKCα, neither the C1A nor the C1B domain of PKCγ is conformationally restricted. Cell studies with enhanced green fluorescent protein-tagged PKCs showed that PKCα did not translocate to the plasma membrane in response to DAG at a basal intracellular calcium concentration due to the inaccessibility of its C1A domain, whereas PKCγ rapidly translocated to the plasma membrane under the same conditions. These data suggest that differential activation mechanisms of PKC isoforms are determined by the DAG affinity and conformational flexibility of their C1 domains.

Protein kinase C (PKC)[1] are a family of serine/threonine kinases that mediate numerous cellular processes (1, 2). All PKCs contain an amino-terminal regulatory domain and a carboxyl-terminal catalytic domain. Based on structural differences in the regulatory domain, PKCs are generally classified into three groups: conventional PKC (α, βI, βII, and γ subtypes), novel PKC (δ, ϵ, η, and θ subtypes), and atypical PKC (ζ and λ/ι subtypes). Regulatory domains of both conventional and novel PKCs contain tandem C1 (C1A and C1B) domains and a C2 domain. The C1 domain (~50 residues) is a cysteine-rich compact structure that contains five short β strands, a short helix, and two zinc ions (3–7), whereas the C2 domain (~130 residues) is composed of eight-stranded antiparallel β strands (5, 8–10) and interconnecting loops some of which are involved in Ca^{2+}-dependent membrane binding. The C1 domain was first identified as the interaction site for diacylglycerol (DAG) and phorbol ester in PKCs (11), but it was subsequently found in other proteins with diverse functions, including protein kinase D (PKD/PKCμ), chimaerin, Ras-GRP, DAG kinases, and Raf-1 kinase (4, 6, 7). In conventional PKCs, C1A and C1B domains are connected to a calcium-binding C2 domain at the carboxyl-terminal side, whereas in novel PKCs a non-calcium binding C2 domain is located at the amino-terminal side of the C1 domains. Roles of C1 and C2 domains in the membrane binding and activation of conventional and novel PKCs have been extensively studied (5, 12). Yet, it is still not fully understood why these PKCs contain two highly homologous C1 domains and what specific roles the two C1 domains play in the membrane binding and activation of the PKCs.

Several laboratories have reported that the two C1 domains of PKCs have disparate ligand affinities and distinct roles (13–19). In particular, Irie *et al.* (20) reported that C1B domains of PKCs have much higher intrinsic affinities for phorbol 12,13-dibutyrate (PDBu) than C1A domains with an exception of PKC-γ whose C1A domain has only modestly lower PDBu affinity than the C1B domain (20). For PKCγ (21) and PKCδ (15), good correlation was observed between the intrinsic phorbol ester affinities of C1A and C1B domains and their relative importance in phorbol ester-induced activation of the full-length proteins, supporting the notion that the disparate roles of C1 domains mainly derive from their different intrinsic affinities for phorbol esters. To date, however, correlation between the intrinsic DAG affinities of C1 domains and their relative importance in DAG-dependent PKC activation has not been documented, which makes it difficult to fully understand the relative contribution of C1A and C1B domains of PKC isoforms to their membrane binding and activation under physiological conditions.

* This work was supported by National Institutes of Health Grants GM52598 and GM53987. The costs of publication of this article were defrayed in part by the payment of page charges. This article must therefore be hereby marked "*advertisement*" in accordance with 18 U.S.C. Section 1734 solely to indicate this fact.

‡ To whom correspondence should be addressed: Dept. of Chemistry (M/C 111), University of Illinois at Chicago, 845 W. Taylor St., Chicago, IL 60607-7061. Tel.: 312-996-4883; Fax: 312-996-2183; E-mail: wcho@uic.edu.

[1] The abbreviations used are: PKC, protein kinase C; DAG, 1,2-*sn*-diacylglycerol; DiC_8, 1,2-*sn*-dioctanoylglycerol; DiC_{18}, 1,2-*sn*-dioleoylglycerol; PDBu, phorbol 12,13-dibutyrate; PMA, phorbol 12-myristate 13-acetate; SPR, surface plasmon resonance; ITC, isothermal titration calorimeter; EGFP, enhanced green fluorescent protein; POPC, 1-palmitoyl-2-oleoyl-*sn*-glycerol-3-phosphocholine; POPS, 1-palmitoyl-2-oleoyl-*sn*-glycerol-3-phosphoserine; PS, phosphoserine; POPG, 1-palmitoyl-2-oleoyl-*sn*-glycerol-3-phosphoglycerol; PG, phosphatidylglycerol; BAPTA-AM, 1,2-bis(2-aminophenoxy)ethane-*N*,*N*,*N*′,*N*′-tetraacetic acid-acetoxymethyl ester.

This study was undertaken to establish the correlation between intrinsic DAG affinity of C1 domains of two conventional PKCs, PKCα and PKCγ, and their relative contribution to the DAG-induced membrane targeting and activation of these PKCs. Determination of affinities of isolated C1A and C1B domains of PKCα and PKCγ for soluble and membrane-incorporated DAG and phorbol ester derivatives by surface plasmon resonance (SPR) analysis and isothermal titration calorimetry (ITC) revealed distinct ligand affinities of these domains. Further studies with full-length PKCα and PKCγ unravel the molecular basis for differential membrane targeting and activation mechanisms of these closely related PKC isoforms.

EXPERIMENTAL PROCEDURES

Materials—1-Palmitoyl-2-oleoyl-*sn*-glycerol-3-phosphocholine (POPC), 1-palmitoyl-2-oleoyl-*sn*-glycero-3-phosphoserine (POPS), 1,2-dioctanoyl-*sn*-glycerol (DiC_8), and 1,2-dioleoyl-*sn*-glycerol (DiC_{18}) were purchased from Avanti Polar Lipids, Inc. (Alabaster, AL) and used without further purification. The Liposofast extruder and 100-nm polycarbonate filters were from Avestin (Ottawa, Ontario, Canada). Phorbol 12,13-dibutyrate (PDBu), phorbol 12-myristate 13-acetate (PMA), fatty acid-free bovine serum albumin, Triton X-100, (3-(3-cholamidopropyl)dimethylammonio)-1-propane sulfonate and octyl glucoside were from Sigma. Pioneer L1 Sensor Chip was from Biacore AB (Piscataway, NJ). Restriction endonucleases and enzymes for molecular biology were obtained from New England Biolabs (Beverly, MA).

Construction of Expression Vectors and Mutagenesis—Expression vectors were constructed by subcloning C1 domain sequences (see Fig. 1) of rat PKCα and PKCγ into pET21d vectors (Novagen, Madison, WI) between NcoI and XhoI sites by overlap extension polymerase chain reaction (PCR) using *Pfu* polymerase (Stratagene, La Jolla, CA). These vectors are designed to introduce a carboxyl-terminal His_6 tag between the XhoI site and stop codon for affinity purification of expressed proteins. Baculovirus transfer vectors encoding the cDNA of PKCα and PKCγ with appropriate C1 domain mutations were generated by the overlap extension PCR using pVL1392 PKCα and PKCγ plasmids, respectively. Briefly, appropriate complementary synthetic oligonucleotides introducing the desired mutation and two other primers at the 5′-end and 3′-end of the genes were used for PCR. Two DNA fragments were then annealed and extended to generate an entire PKC gene containing a desired mutation, which was further amplified by PCR. The product was subsequently purified on an agarose gel, digested with NotI and EcoRI for PKCα and with BglII and EcoRI for PKCγ, and the corresponding restriction fragments were subcloned into the pVL1392 plasmid. The mutagenesis was verified by DNA sequencing using a Sequenase 2.0 kit (Amersham Biosciences).

Protein Expression and Purification—Escherichia coli strain BL21(DE3) (Novagen) was used as host for C1 domain expression. One liter of Luria-Bertani medium supplemented with 100 μg/ml ampicillin was inoculated with 1 ml of overnight culture grown at 37 °C. Cells were grown at 37 °C until their absorbance at 600 nm reached ~0.8–1.4, and the protein expression was then induced with 0.5 mM isopropyl-1-thio-β-D-galactopyranoside (Research Products, Mount Prospect, IL). After 4 h, cells were harvested by centrifugation (5,000 × *g* for 10 min at 4 °C). Cells were resuspended in 20 ml of lysis buffer containing 50 mM Tris-HCl, pH 7.4, 50 mM NaCl, 0.4% (v/v) Triton X-100, and 1 mM phenylmethylsulfonyl fluoride, and sonicated. The supernatant was collected by centrifugation at 50,000 × *g* for 25 min at 4 °C. The C1B domains of PKCα and PKCγ were expressed as soluble proteins, whereas others form inclusion bodies. Soluble C1 domains were purified from the supernatant using a nickel-nitrilotriacetic acid (Qiagen) column according to the manufacturer's instructions. On the other hand, insoluble proteins were recovered from the inclusion body pellet, refolded, and purified. First, the inclusion body pellet was resuspended in the same lysis buffer and re-centrifuged at 50,000 × *g* for 25 min at 4 °C. The washed inclusion body was resuspended in 10 ml of 50 mM Tris-HCl, pH 8.0, containing 50 mM NaCl, 8 M urea, and 5 mM dithiothreitol. Insoluble matter was removed by centrifugation at 100,000 × *g* for 15 min, and the supernatant was dialyzed against 50 mM Tris-HCl, pH 8.0, containing 50 mM NaCl, 1.5 M urea, 50 μM $ZnSO_4$, and 0.5 mM dithiothreitol, and then against 50 mM Tris-HCl, pH 8.0. The refolded C1 domain was purified using a nickel-nitrilotriacetic acid column (Qiagen) according to the manufacturer's instructions. The resulting protein was dialyzed against 50 mM Tris-HCl, pH 8.0, to remove the imidazole. Purity of C1 domain samples was higher than 90% electrophoretically.

Full-length PKCα and PKCγ proteins were expressed in baculovirus-infected Sf9 cells (Invitrogen, La Jolla, CA) as described previously (22). Transfection of Sf9 cells with pVL1392-based PKC constructs was performed using BaculoGold™ Transfection kit from BD Pharmingen (San Diego, CA). Prior to transfection, endotoxins were removed from the plasmid DNA using a lipopolysaccharide extraction kit (Qiagen, Valencia, CA). Cells were incubated for 4 days at 27 °C, and the supernatant was collected and used to infect more cells for the amplification of virus. After three cycles of amplification, high titer virus stock solution was obtained. Sf9 cells were maintained as monolayer cultures in Grace's insect cell culture medium (Invitrogen) containing 10% fetal bovine serum (Invitrogen). For protein expression, cells were grown to 2×10^6 cells/ml in 500-ml suspension cultures and infected with the multiplicity of infection of 10. The cells were then incubated for 3 days at 27 °C. For harvesting, cells were centrifuged at 1000 × *g* for 10 min, washed once with Tris-HCl buffer, pH 7.4, and resuspended in 25 ml of extraction buffer containing 20 mM Tris-HCl, pH 7.4, 2 mM EGTA, 2 mM EDTA, 1 mM dithiothreitol, 50 μg/ml leupeptin, 1% Triton X-100, and 0.2 mM phenylmethylsulfonyl fluoride. The suspension was homogenized in a hand-held homogenizer chilled on ice. The extract was centrifuged at 50,000 × *g* and at 4 °C for 40 min. The supernatant was loaded onto a 100-ml Q-Sepharose Fast Flow column (Amersham Biosciences). After washing with 100 ml of Buffer A (20 mM Tris-HCl, pH 7.4, 1 mM dithiothreitol), the column was eluted with 200 ml of a linear salt gradient to 0.5 M KCl in Buffer A. Active PKC fractions were pooled, adjusted to 2 M KCl, and loaded onto a 10-ml Poros PE column (Roche Applied Science) with a flow rate of 4 ml/min. A linear salt gradient from 2 to 0 M KCl in Buffer A (total volume, 60 ml) was applied. Active PKC fractions were concentrated and desalted in an Ultrafree-15 centrifugal filter device (Millipore) and stored in Buffer A containing 50% glycerol at −20 °C. Purity of the full-length proteins was higher than 80% electrophoretically. Protein concentration was determined by the bicinchoninic acid method (Pierce).

PKC Activity Assay—Activity of PKC was assayed by measuring the initial rate of [^{32}P]phosphate incorporation from [γ-^{32}P]ATP (50 μM, 0.6 μCi/tube) into the histone III-SS (400 μg/ml) (Sigma). The reaction mixture contained large unilamellar vesicles (0.1 mM), 5 mM $MgCl_2$, PKC, and 0.1 mM $CaCl_2$ in 50 μl of 20 mM Tris-HCl, pH 7.4. Free calcium concentration was adjusted using a mixture of EGTA and $CaCl_2$ according to the method of Bers (23). Reactions were started by adding $MgCl_2$ to the mixture and quenched by adding 50 μl of 1% aqueous phosphoric acid solution after a given period of incubation (5 min for PKCα and 10 min for PKCγ) at room temperature. 75-μl aliquots of quenched reaction mixtures were spotted on P-81 ion-exchange papers (Whatman), washed four times with 1% aqueous phosphoric acid solution, and washed once with 95% aqueous ethanol. Papers were transferred into scintillation vials containing 4 ml of scintillation fluid (Sigma), and radioactivity was measured by liquid scintillation counting. The linearity of the time dependence of the reaction was checked by monitoring the degree of phosphorylation at regular intervals.

SPR Measurements—The preparation of vesicle-coated Pioneer L1 sensor chip (Biacore) was described in detail elsewhere (24). Briefly, after washing the sensor chip surface, 90 μl of vesicles containing POPC/POPS/DiC_{18} (67.5:30:2.5 in mole ratio) or POPC/POPS/PMA (70:30:0.05) were injected at 5 μl/min. Similarly, a control surface was coated with POPC vesicles to give the same resonance unit response as the active binding surface. This control surface was selected over the bare chip surface to circumvent any potential artifacts caused by the hydrophobic nature of the L1 chip. Each lipid layer was stabilized by injecting 10 μl of 50 mM NaOH until no decrease in lipid signal was observed. After the signal was stabilized, 90 μl of protein in 20 mM Tris-HCl, pH 7.4, containing 0.16 M KCl and 50 μM $ZnSO_4$ was injected. Due to extremely slow dissociation of C1 domains from the vesicle surface, it was impractical to determine K_d from kinetic measurements. Hence, equilibrium binding measurements were performed with the flow rate of 5 μl/min to allow sufficient time for the R values of the association phase to reach saturating response values (R_{eq}). R_{eq} values were then plotted *versus* protein concentrations (C), and the K_d value was determined by a non-linear least-squares analysis of the binding isotherm using an equation, $R_{eq} = R_{max}/(1 + K_d/C)$.

ITC Measurements—Binding of C1 domains to water-soluble PDBu or DiC_8 ligands was measured using a MicroCal VP isothermal titration calorimeter (MicroCal Inc., Northampton, MA). Protein samples used for the titration were prepared by dialyzing overnight against 4 liters of a working buffer (20 mM Tris-HCl, pH 7.4, 0.16 M KCl, 50 μM $ZnSO_4$). Experiments were performed at 30 °C using the working buffer as a reference and a diluent. Protein concentration and ligand concentration used for each measurement varied according to the range of K_d value to be measured. Binding measurements were performed with 5-μl step-

```
                                    55  58 60
PKCαC1a    HKFIARFFKQPTFCSHCTDFIWGFGKQGFQCQVCCFVVHKRCHEFVTFSC
PKCγC1a    HKFTARFFKQPTFCSHCTDFIWGIGKQGLQCQVCSFVVHRRCHEFVTFEC

                                116         123 125
PKCαC1b    HKFKIHTYGSPTFCDHCGSLLYGLIHQGMKCDTCDMNVHKQCVINVPSLC
PKCγC1b    HKFRLHSYSSPTFCDHCGSLLYGLVHQGMKCSCCEMNVHRRCVRSVPSLC
```

FIG. 1. **Amino acid sequence alignment of C1A and C1B domains of PKCα and PKCγ.** Mutated residues are highlighted in *boldface characters*. Numbering is based on the residue number of PKCα.

wise injections of the ligand into the protein in the sample cell. Injections were continued until saturating signals were obtained. The collected data were analyzed with the Origin software (MicroCal) using a simple single-site binding model.

Monolayer Measurements—The penetration of PKC into the phospholipid monolayer was measured by monitoring the change in surface pressure (π) at constant surface area using a 10-ml circular Teflon trough and Wilhelmy plate connected to a Cahn microbalance as previously described (25). All our monolayer measurements were performed at 23 °C. A lipid monolayer containing various combinations of phospholipids was spread onto the subphase composed of 10 mM Tris-HCl, pH 7.4, containing 0.16 M KCl until the desired initial surface pressure (π_0) was reached. After the signal stabilized (~5 min), 30 μg of proteins was injected, and the increase in surface pressure ($\Delta\pi$) was monitored for 45 min while stirring the subphase at 60 rpm. Typically, the $\Delta\pi$ value reached a maximum after 20 min. It has been shown empirically that $\Delta\pi$ caused by a protein is mainly due to the penetration of the protein into the lipid monolayer (25). The maximal $\Delta\pi$ value depended on the protein concentration and reached a saturation value (*e.g.* [PKCα] $\geq$ 2.0 μg/ml); therefore, the protein concentration in the subphase was maintained above such values to ensure that the observed $\Delta\pi$ represented a maximum value. The resulting $\Delta\pi$ was plotted *versus* π_0 from which the critical surface pressure (π_c) was determined as the *x*-intercept (26).

Cell Culture—A stable HEK293 cell line expressing the ecdysone receptor (Invitrogen) was used for all experiments. Briefly, cells were cultured in Dulbecco's modified Eagle's medium supplemented with 10% fetal bovine serum at 37 °C in 5% CO_2 and 98% humidity until 90% confluent. Cells were passaged into eight wells of a Lab-Tech™ chambered coverglass for later transfection and visualization. Cells between the 5th and 20th passages were used for all measurements. For transfection, 80–90% confluent cells in Lab-Tech™ chambered coverglass wells were exposed to 150 μl of unsupplemented Dulbecco's modified Eagle's medium containing 0.5 μg of endotoxin-free DNA and 1 μl of LipofectAMINE™ reagent (Invitrogen) for 7 h at 37 °C. After exposure, the transfection medium was removed, the cells were washed once with fetal bovine serum-supplemented Dulbecco's modified Eagle's medium, and overlaid with fetal bovine serum-supplemented Dulbecco's modified Eagle's medium containing Zeocin™ (Invitrogen) and 5 μg/ml ponasterone A (Invitrogen) to induce protein production.

Confocal Microscopy—All imaging was done using a four-channel Zeiss LSM 510 laser scanning confocal microscope. A 63×, 1.2-numerical aperture water immersion objective was used for all experiments, which were carried out at the same laser power and the same gain and offset settings on the photomultiplier tubes. These conditions induced minimal photobleaching over 45 scans. EGFP was excited using the 488-nm line of an argon/krypton laser, and a linepass 505-nm filter was used to monitor EGFP emission. To clamp intracellular Ca^{2+} ($[Ca^{2+}]_i$) cells were loaded with 10 μM BAPTA-AM (Molecular Probes, Eugene, OR) 30 min prior to imaging. Immediately before imaging, cells were washed with 150 μl of 1 mM EGTA, followed by a washing with 150 μl of HEK buffer (1 mM HEPES, pH 7.4, containing 6 mM sucrose, 140 mM NaCl, 5 mM KCl, 2.5 mM $MgCl_2$) and then overlaid with 150 μl of HEK buffer. After initially imaging cells, protein translocation was monitored by scanning at 8- to 15-s intervals following addition of 0.1 μg/μl DiC_8 (final concentration). Treatment of cells with 1% Me_2SO alone did not induce translocation of PKCα or -γ. Control experiments done with HEK293 cells loaded with Fura Red (Molecular Probes) indicated that addition of DiC_8 to HEK293 cells do not increase $[Ca^{2+}]_i$, precluding the possibility that the translocation response in these experiments is due to an increase in $[Ca^{2+}]_i$.

Images were analyzed as described previously (27) using the analysis tools provided in the Zeiss biophysical software package. Briefly, regions of interest in the cytosol were defined, and the average intensity in a square (1 × 1 μm) was obtained with respect to time. Membrane intensities were determined for each frame in individual cells by extending a line from the cytosol to the outside of the cell and recording the intensity with distance along the line. By crosschecking markers on the diagram with a table of intensity data, three intensity values corresponding to the place on the line indicating the edge of the cell were averaged. Lines were drawn in three places in each cell, and membrane intensity values were determined and averaged. The resulting intensity values were converted to a ratio of intensity at the membrane to the sum of intensities at the membrane and at the cytosol for each time frame. A plot of this intensity ratio *versus* time was prepared to visualize and compare the translocation response for wild type and mutant proteins.

RESULTS

Functional Expression and Characterization of C1 Domains—We selected for this study the C1 domains of two conventional PKCs, PKCα and PKCγ, for two reasons. First, our previous studies indicated that only the C1A domain plays a critical role in the DAG-induced membrane binding and activation of PKCα (17, 18). It is not known, however, whether or not this exclusive role of the C1A domain is due to its higher intrinsic affinity for DAG than the C1B domain. Second, unlike other PKC isoforms, PKCγ has been shown to have two C1 domains with comparable phorbol ester affinity (20). This raises an interesting possibility that the two C1 domains of PKCγ might also have similar DAG affinity and therefore contribute similarly to the membrane binding and activation of this PKC isoform. Therefore, these two homologous PKC isoforms should serve as an excellent model to test how DAG affinity of individual C1 domains affects the membrane binding and activation mechanism of PKCs.

We first expressed and characterized the C1A and C1B domains of PKCα and PKCγ whose amino acid sequences are shown in Fig. 1. PKC C1 domains have aliphatic and aromatic side chains surrounding the ligand binding pocket that have been shown to be involved in membrane insertion and hydrophobic membrane interactions (3, 17, 18, 28). Due to the presence of these exposed hydrophobic residues, C1 domains have a high tendency to aggregate when they are ectopically expressed in bacterial cells (29), hampering their functional expression. In fact, C1B domains were expressed as soluble proteins in *E. coli* with relatively low yield (<1 mg/liter of culture medium), whereas C1A domains were expressed as inclusion bodies. The latter proteins were then solubilized in urea and refolded. To verify that all the C1 domains were functionally folded, their affinity for PDBu was measured by ITC and compared with the reported values. Fig. 2 shows a representative ITC binding isotherm for the C1B domain of PKCγ with PDBu, and the values of K_d and stoichiometry determined from data analysis are summarized in Table I. Taking into account the fact that completely different assays were used for affinity determination and that our C1 domain constructs and the reported ones have different size, reasonable agreement between our K_d values and reported values (20) indicate that our C1 domains are functionally folded. Most notably, the C1A domain of PKCα has no detectable affinity for PDBu, whereas the C1A domain of PKCγ has only 5-fold lower affinity than its C1B domain for PDBu.

We then determined the affinity of these domains for a short-chain DAG analog, DiC_8, by ITC analysis (see Table II for the K_d and stoichiometry values). DiC_8 should exist as a mon-

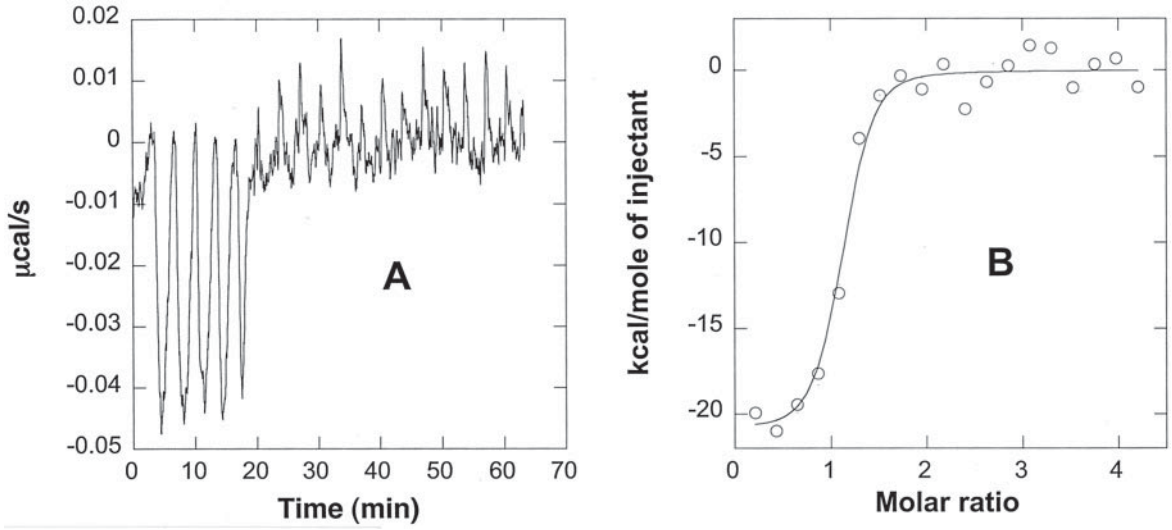

FIG. 2. **ITC binding isotherm for PKCγ C1B domain and PDBu.** *A*, raw data in terms of μcal/s plotted against time (min), after the integration baseline has been subtracted. *B*, normalized integration data in terms of kcal/mol of injectant plotted against molar ratio of lipid to protein. The non-linear least-squares curve fitting was performed with the Origin (MicroCal) software using a single-site binding model.

TABLE I

Phorbol ester binding parameters for PKCα and PKCγ C1 domains determined from ITC and SPR analyses

Values represent the mean and S.D. from three determinations. All measurements were performed in 20 mM Tris-HCl, pH 7.4, containing 0.16 M KCl and 50 μM $ZnSO_4$ unless specified otherwise.

Protein	PDBu (literature)[a] K_d	PDBu (ITC analysis)		PMA[b] (SPR analysis) K_d
		Stoichiometry	K_d	
	nM	*N*	*nM*	*nM*
PKCα C1A	>3,000	NM[c]	NM[c]	121.0 ± 26.2
PKCα C1B	46.7	0.80 ± 0.03	21.4 ± 5.0	6.3 ± 1.5
PKCγ C1A	65.8	0.94 ± 0.05	51.9 ± 17.0	1.9 ± 0.3
PKCγ C1B	16.9	1.03 ± 0.02	9.3 ± 3.8	1.7 ± 0.5

[a] Taken from Ref. 20.
[b] POPC/POPS/PMA (69.95:30:0.05 in mole ratio) vesicles.
[c] NM, not measurable.

TABLE II

Diacylglycerol binding parameters for PKCα and PKCγ C1 domains determined from ITC and SPR analyses

Values represent the mean and S.D. from three determinations. All measurements were performed in 20 mM Tris-HCl, pH 7.4, containing 0.16 M KCl and 50 μM $ZnSO_4$ unless specified otherwise.

Protein	DiC_8 (ITC analysis)		DiC_{18} (SPR analysis)[a] K_d
	Stoichiometry	K_d	
	n	*nM*	*nM*
PKCα C1A	0.89 ± 0.04	10.2 ± 3.1	3.6 ± 0.5
PKCα C1B	NM[b]	NM[b]	2700.0 ± 710.0
PKCγ C1A	0.84 ± 0.08	10.4 ± 5.0	5.5 ± 1.0
PKCγ C1B	1.07 ± 0.04	8.9 ± 3.1	5.2 ± 0.6

[a] POPC/POPS/DiC_{18} (67.5:30:2.5 in mole ratio) vesicles.
[b] NM, not measurable.

omer in the concentration range (10–100 nM) used for this binding study, because its critical micellar concentration was estimated to be ~15 μM by the surface tension measurement.[2] Intriguingly, the C1A domain of PKCα and the two C1 domains of PKCγ all have comparably high affinity for DiC_8, whereas the C1B domain of PKCα has no detectable affinity. Thus, it is evident that the C1A and C1B domains of PKCα have opposite affinities for DAG and phorbol ester; *i.e.* the C1A domain with high affinity for DAG and the C1B domain with high affinity for phorbol ester. These data show that the predominant role of the C1A domain in the DAG-induced membrane binding and activation of PKCα derives at least in part from its high DAG affinity. These data also suggest that both the C1A and C1B domains might be actively involved in the DAG-induced membrane binding and activation of PKCγ, because they have comparable DAG affinity.

We also measured the binding of the C1 domains to DAG and phorbol ester with longer acyl chains that are incorporated in the lipid bilayer. First, we measured the affinity of the C1 domains for POPC/POPS/DiC_{18} (67.5:30:2.5 in mole ratio) vesicles by SPR analysis, which has been shown to be a powerful tool for measuring membrane-protein binding (24, 26, 30, 31). Fig. 3 shows typical sensorgrams and data analysis for the C1A domain of PKCγ. As shown in Table II, the C1B domain of PKCα exhibited lower affinity for the DAG-containing vesicles than other three C1 domains by about three orders of magnitudes. These data thus show that the C1A domain of PKCα has much higher affinity for DAG, whether it is in solution or in the

[2] B. Ananthanarayanan and W. Cho, unpublished observation.

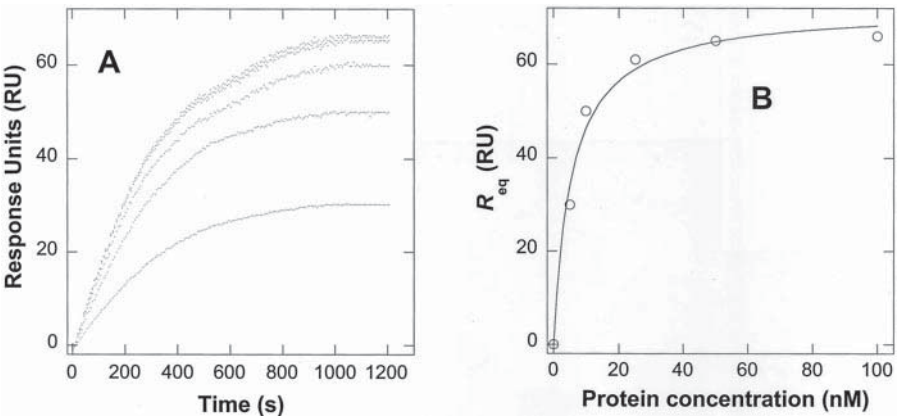

FIG. 3. **Determination of K_d for PKCγ C1A domain-DiC$_8$ binding by SPR analysis.** *A*, varying concentrations of protein (5, 10, 25, 50, and 100 nM) was injected at 5 μl/min to obtain R_{eq} values. *B*, R_{eq} values were then plotted *versus* protein concentrations. A *solid line* represents a theoretical curve constructed from R_{max} (72 ± 3) and K_d (5.5 ± 1.0 nM) values determined by non-linear least-squares analysis of the isotherm using an equation, $R_{eq} = R_{max}/(1 + K_d/C)$.

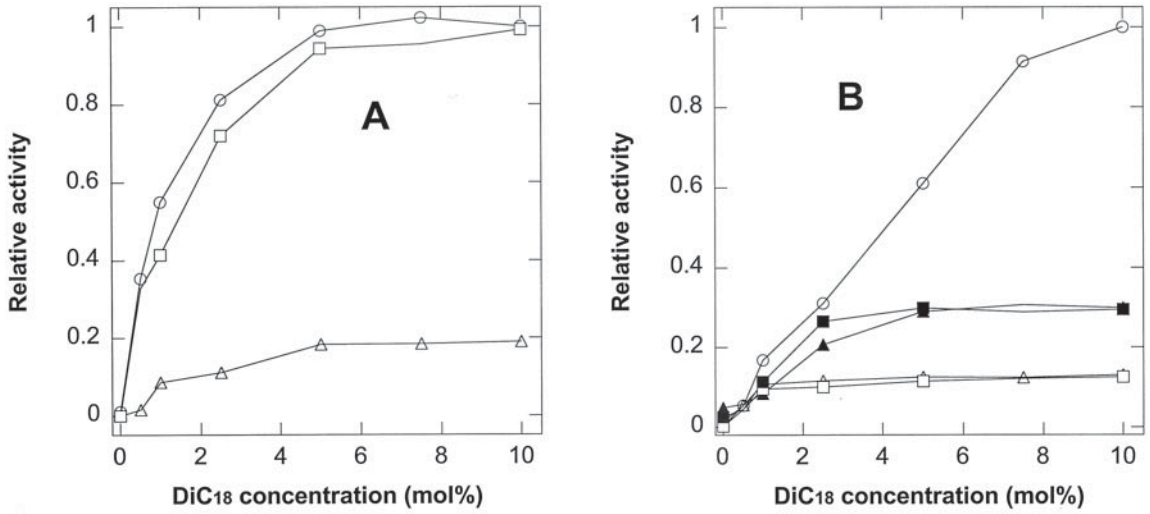

FIG. 4. **Dependence of enzymatic activity of PKCs on DiC$_{18}$ concentration.** *A*, activity of PKCα wild type (○), W58A (△), and Y123A (□) was measured in POPC/POPS/DiC$_{18}$ (70-*x*:30:*x*) vesicles. Relative activity was calculated as the ratio of the maximal activity of PKCα (20 nmol/mg·min) to a given activity value. *B*, activity of PKCγ wild type (○), W58A (△), I60A (▲), Y123A (□), and L125A (■) was measured in POPC/POPS/DiC$_{18}$ (70-*x*:30:*x*) vesicles. Relative activity was calculated as the ratio of the maximal activity of PKCγ (3 nmol/mg·min) to a given activity value.

membrane, whereas the two C1 domains of PKCγ have comparable affinity for DAG. Second, we measured the binding of the C1 domains to POPC/POPS/PMA (69.95:30:0.05 in mole ratio) vesicles. In accordance with their PDBu affinity, the C1A domain of PKCα has ~20-fold lower affinity for the PMA-containing vesicles than its C1B domain, whereas the two C1 domains of PKCγ have comparable affinity for the same vesicles. This again shows that these C1 domains have similar relative affinity for phorbol esters, whether they are in solution or in the membrane, although the difference in their affinity is smaller for the membrane-incorporated phorbol ester.

Differential Roles of C1A and C1B Domains of PKCα and PKCγ—We previously reported that the mutations of hydrophobic residues (Trp^{58} and Phe^{60}) in the C1A domain of PKCα had a much greater effect on the DAG-induced membrane binding and activation of this PKC isoform than those of corresponding hydrophobic residues (Tyr^{123} and Leu^{125}) in the C1B domain (17). These results, along with other data (18), led us to propose a mechanism for PKCα activation in which the C2 domain initially brings the protein to the membrane surface, which is followed by the membrane penetration and DAG binding of the C1A domain. The latter leads to the removal of the pseudosubstrate region from the active site and the enzyme activation. Our finding that the C1A and C1B domains of PKCγ have comparable affinity for DAG suggested that this conventional PKC isoform might have a distinct activation mechanism in which both C1A and C1B domains contribute equally to the membrane penetration and DAG binding, and eventually enzyme activation. To test this notion, we mutated hydrophobic residues of C1A (Trp^{58} and Ile^{60}) and C1B (Tyr^{123} and Leu^{125}) domains of PKCγ, respectively, and measured the effects of mutations on enzyme activity. Trp^{58} in the C1A domain occupies the same site as Tyr^{123} in the C1B domain, whereas Ile^{60} in the C1A domain corresponds to Leu^{125} in the C1B domain (see Fig. 1). For comparison, we also measured the properties of corresponding mutants of PKCα. Fig. 4 shows the relative enzyme activity of PKCα, PKCγ, and their mutants as a function of DiC$_{18}$ concentration in POPC/POPS/DiC$_{18}$ (70-*x*:30:*x*) vesicles. For PKCα, a C1A domain mutation (W58A) had a drastic effect on PKC activity, whereas a C1B domain mutation (Y123A) showed little effect, which is consistent with our previous report (17). In contrast, C1A and C1B mutations exerted similar effects on the PKCγ activity, supporting the notion that the C1A and C1B domains contribute equally to the membrane binding and activation of PKCγ. Intriguingly, the mutations of Trp^{58} of the C1A domain and Tyr^{123} of the C1B domain had

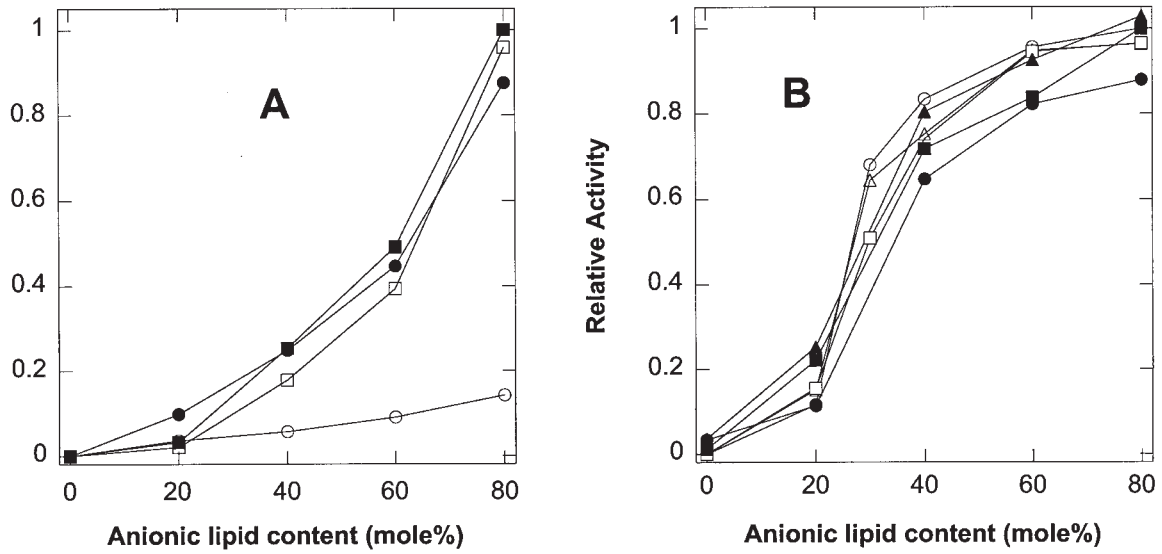

FIG. 5. **Dependence of enzymatic activity of PKCs on anionic lipid concentration.** *A*, activity of PKCα wild type (○/●) and D55A (△/▲) was measured in POPC/POPS/DiC_{18} (67.5-*x*:*x*:2.5) vesicles (*filled symbols*) and POPC/POPG/DiC_{18} (67.5-*x*:*x*:2.5) vesicles (*open symbols*). Relative activity was calculated as the ratio of the maximal activity of PKCα (28 nmol/mg·min) to a given activity value. *B*, activity of PKCγ wild type (○/●), D55A (△/▲), and D116A (□/■) was measured in POPC/POPS/DiC_{18} (67.5-*x*:*x*:2.5) vesicles (*open symbols*) and POPC/POPG/DiC_{18} (67.5-*x*:*x*:2.5) vesicles (*filled symbols*). Relative activity was calculated as the ratio of the maximal activity of PKCγ (4.3 nmol/mg·min) to a given activity value.

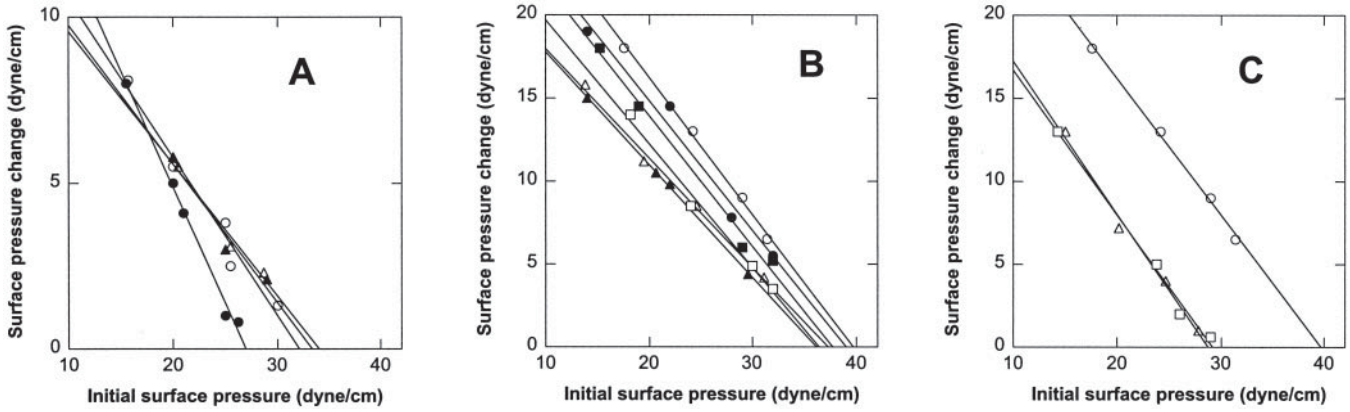

FIG. 6. **Monolayer penetration of PKCα, PKCγ, and mutants.** *A*, $\Delta\pi$ was measured as a function of π_0 for PKCα wild type (○/●), and D55A (△/▲) with POPC/POPS (7:3) (*open symbols*) and POPC/POPG (7:3) (*filled symbols*) monolayers. *B*, $\Delta\pi$ was measured as a function of π_0 for PKCγ wild type (○/●), D55A (△/▲), and D116A (□/■) with POPC/POPS (7:3) (*open symbols*) and POPC/POPG (7:3) (*filled symbols*) monolayers. *C*, the penetration of PKCγ wild type (○), W58A (△), and Y123A (□) into the POPC/POPS (7:3) monolayer.

larger effects than the mutations of Ile^{60} and Leu^{125}. These data suggest that the C1A and C1B domains of PKCγ might interact with the membrane in essentially the same manner with Trp^{58} and Tyr^{123} making direct contact with the membrane and with Ile^{60} and Leu^{125} less directly involved in membrane binding. Furthermore, almost complete inactivation of PKCγ by the single W58A or Y123A mutation, *i.e.* lack of compensation by the other C1 domain, indicates that both domains are required for the DAG-induced activation of PKCγ. This inactivation is unlikely to be due to deleterious conformational changes caused by mutations, because W58A and Y123A showed the wild type-like activity when protamine sulfate was used as substrate, for which PKCs require no lipid cofactors. The notion that both C1A and C1B domains are required for DAG-induced activation of PKCγ is also consistent with the finding that the full activation of PKCγ requires about twice more DiC_{18} than that of PKCα under the same conditions (Fig. 4). Notice that the C1A domain of PKCα and the C1A and C1B domains of PKCγ all have essentially the same intrinsic DAG affinity. Although an attempt to directly determine the DAG binding stoichiometry of full-length PKCα and PKCγ by ITC analysis was hampered by the requirement of prohibitively large amounts of pure proteins, these data suggest that the activation of PKCα involves the binding of a single DAG molecule to its C1A domain, whereas the activation of PKCγ occurs through the binding of two DAG molecules to its C1A and C1B domains, respectively.

Differential Activation Mechanisms of PKCα and PKCγ—We previously showed that Asp^{55} in the C1A domain of PKCα is involved in tethering of the C1A domain to the other part of the PKC molecule (18), presumably its C2 domain (32). It was postulated that the PS specificity of PKCα activation derives from the release of the tethering by PS that binds to the C2 domain (and possibly other parts) of PKCα. Isolated C2 domains of both PKCα and PKCγ were shown to have comparably affinity for PS (33). However, the finding that C1 domains of PKCα and PKCγ play distinct roles in the DAG-induced membrane binding and activation of these PKCs implied that the PS binding might exert different effects on their activation. To test this notion, we first measured the PS dependence of PKCα and PKCγ activity. Specifically, we measured the activity of PKCα and PKCγ in the presence of POPC/POPS/DiC_{18} (67.5-*x*:*x*:2.5)

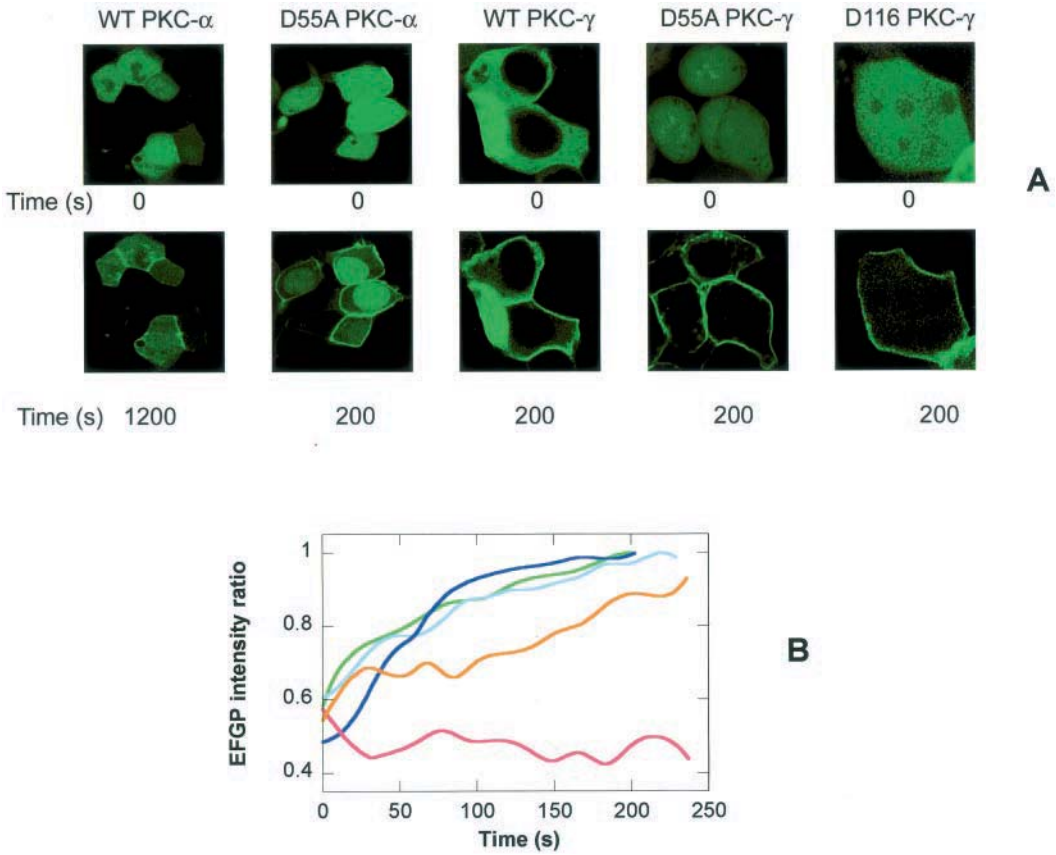

FIG. 7. **Membrane translocation of EGFP-tagged PKCα, PKCγ, and mutants in response to DiC_8 treatment.** *A*, cells preincubated with BAPTA-AM were treated with 0.1 mg/ml DiC_8, and confocal images were taken every 10 s. Images before and 200 s (20 min for PKCα wild type) after the addition of DiC_8 are shown. *B*, the time-lapse changes in EGFP intensity ratio at the plasma membrane (= plasma membrane/[plasma membrane + cytoplasm]) are shown for for PKCα wild type (*red*), PKCα D55A (*orange*), PKCγ wild type (*blue*), PKCγ D55A (*green*), and PKCγ D116A (*cyan*).

and POPC/POPG/DiC_{18} (67.5-*x*:*x*:2.5) vesicles. As shown in Fig. 5, the PKCα activity was highly dependent on the presence of PS in the vesicles. By contrast, PKCγ showed high relative activity in the presence of both PS and PG vesicles; consequently, it had much reduced PS selectivity than PKCα. In this regard, PKCγ is reminiscent of the D55A mutant of PKCα that was shown to have enhanced activity in the presence of both PS and PG vesicles because of disruption of interdomain tethering by the mutation (18). This in turn suggested that the C1 domains of PKCγ are not tethered and can thus readily bind their cognate ligands. Consistent with this notion, both the D55A mutant and the D116A mutant (a C1B domain counterpart of D55A) of PKCγ behaved like the wild type in the activity assay. It would seem that the lower specific activity of PKCγ wild type compared with that of PKCα wild type is at odds with the notion that the C1 domains of PKCγ can bind DAG more readily than the C1A domain of PKCα. It should be noted, however, that the *in vitro* enzyme assay was performed with high concentration (*i.e.* 0.1 mM) of Ca^{2+}, which allows full mobilization of the C1A domain of PKCα (18), and that histone used for all activity assays is an excellent substrate for PKCα but is a suboptimal PKCγ substrate (34, 35).

To provide further evidence for the notion that the C1 domains of PKCγ are less conformationally restricted than the C1A domain of PKCα, we measured the penetration of PKCα, PKCγ, and their respective mutants into lipid monolayers. Lipid monolayers at the air-water interface serve as a highly sensitive tool to measure the membrane-penetrating ability of protein (26, 36). In these studies, POPC/POPS (70:30) and POPC/POPG (70:30) monolayers of a given initial surface pressure (π_0) were spread at constant area and the change in surface pressure ($\Delta\pi$) was monitored after the injection of the protein into the subphase. DAG was not included in the lipid monolayers, because DAG itself was shown to have no effect on the monolayer insertion of PKCs (22, 37, 38). In general, $\Delta\pi$ is inversely proportional to π_0 of the lipid monolayer and an extrapolation of the $\Delta\pi$ *versus* π_0 plot yields the critical surface pressure (π_c), which specifies an upper limit of π_0 of a monolayer that a protein can penetrate into (26, 36). Because the surface pressure of cell membranes has been estimated to be in the range of 30–35 dyne/cm (39–41), for a protein to penetrate these membranes its π_c value should be above 30 dyne/cm. Fig. 6 illustrates the penetration of PKCα, PKCγ, and their mutants into POPC/POPS (7:3) and POPC/POPG (7:3) monolayers. As reported previously (18), PS specifically enhanced the π_c of PKCα above 30 dyne/cm, and its D55A mutant had a high π_c value even in the presence of a nonspecific lipid, POPG (Fig. 6*A*). This was interpreted as an indication that PS specifically disrupts the interdomain tethering via Asp^{55} and thereby allows the C1A domain to partially penetrate the cell membrane and bind DAG that is located near the hydrophobic core of the membrane due to its hydrophobic nature (18). Fig. 6*B* demonstrates that PKCγ has a distinctly different monolayer penetration behavior: PKCγ showed much higher membrane penetration activity (*i.e.* higher π_c) than PKCα in the presence of both PS and PG in the monolayer. This high monolayer penetration activity of PKCγ was due to the monolayer penetration of hydrophobic residues in the C1A and C1B domain, because both W58A and Y123A mutations significantly reduced the π_c of the wild type (Fig. 6*C*). Furthermore, neither D55A nor D116A mutation had a significant positive effect on the monolayer penetration of PKCγ (Fig. 6*B*). In fact, both mutations

slightly reduced the monolayer penetration of PKCγ. Collectively, these data are consistent with the notion that PKCγ does not require PS for activation, because neither the C1A domain nor the C1B domain is conformationally restricted in PKCγ.

Cellular Membrane Translocation of PKCα and PKCγ—To see if different *in vitro* membrane-binding properties of PKCα and PKCγ also govern their cellular membrane targeting, we transfected HEK293 cells with PKCα, PKCγ, and their mutants, each tagged with EGFP in the carboxyl-terminal end. The *in vitro* SPR assay showed that PKCα or PKCγ with the EGFP tag at the carboxyl terminus had the affinity for POPC/POPS/DiC_{18} (67.5:30:2.5) vesicles that was comparable (*i.e.* less than 5% difference) to their amino-terminal His_6-tagged counterparts employed for the *in vitro* studies (data not shown). Also, the level of cellular expression of different protein constructs was comparable in most cells, when assessed by Western blotting using PKC-specific antibodies (data not shown).

Membrane translocation of EGFP-tagged PKCs was induced by treating the transfected cells with DiC_8. Intracellular calcium concentration ($[Ca^{2+}]_i$) was reduced to <100 nM by pretreating the cells with BAPTA-AM. This condition was employed because at higher $[Ca^{2+}]_i$, the C2 domain plays a major role in the membrane translocation of conventional PKCs, which makes it difficult to sort out the contribution of C1 domains and C2 domain to membrane translocation of PKCα and PKCγ. Confocal images of PKC before and after cell stimulation with DiC_8 are shown in Fig. 7*A*, and the time-lapse change of relative EFGP intensity at the plasma membrane is shown in Fig. 7*B*. In this study, high concentration (0.1 mg/ml) of DiC_8 was employed to ensure that the cellular turnover of DiC_8 level would not significantly reduce the PKC translocation during the confocal measurements. Fig. 7 demonstrates that PKCα did not move to the plasma membrane for up to 20 min after DiC_8 treatment, which is consistent with the notion that the C1A domain of PKCα is not accessible for DAG binding in its resting state. This notion is further supported by the finding that the D55A mutant of PKCα, whose C1A domain was shown to have much greater conformational flexibility than that of wild type (18), readily translocated to the plasma membrane under the same conditions. In contrast to PKCα, PKCγ rapidly migrated to the plasma membrane in response to DiC_8. In the case of PKCγ, neither D55A nor D116A mutation had an appreciable effect on the membrane translocation of the protein, which is consistent with our *in vitro* finding that both C1A and C1B domains of this PKC isoform are accessible for DAG binding even in the resting state.

DISCUSSION

Despite extensive studies on PKCs, it is still not fully understood how differently individual PKC isoforms bind the membrane and get activated. In particular, determination of the roles of the two C1 domains in the activation of conventional and novel PKCs has been elusive. To address this question, the phorbol ester affinity of many C1 domains has been determined, which revealed that all C1A domains except that of PKCγ have very low affinity for PDBu (20). This is because C1A domains lack residues that are involved in specific phorbol ester recognition. Surprisingly, however, quantitative determination of the affinity of PKC C1 domains for their physiological ligand, DAG, has not been reported to date. The lack of this information has made it difficult to rationalize the potentially differential roles of C1A and C1B domains in the DAG-induced PKC activation in the cell. Due to experimental convenience, the cellular membrane binding and activation of PKC isoforms has been mainly studied in the presence of a non-physiological activator, phorbol ester. Our finding that the C1A and C1B domains of PKCα have opposite affinities for DAG and phorbol esters, which was also suggested in previous spectroscopic studies (14, 42), demonstrate that the principles learned from the phorbol ester-mediated activation of a PKC isoform may not be applied to the DAG-mediated activation of the PKC.

In this study two conventional PKCs, PKCα and PKCγ, were selected because the mechanism of the DAG-induced membrane targeting and activation of PKCα is relatively well understood and because PKCγ uniquely contains two C1 domains with comparable phorbol ester affinity. Based on extensive structure-function studies on PKCα, we proposed a mechanism for its activation (17, 18). In this mechanism, membrane binding of PKCα is initially driven by electrostatic interactions involving the C2 domain-bound calcium ions and cationic residues in the C1A domain. The C1A domain is normally tethered to other part(s) (presumably the C2 domain) (32) of the protein via Asp^{55} and unavailable for DAG binding. This putative tethering is released by PS, whose carboxyl group in the headgroup might replace Asp^{55}, thereby allowing the C1A domain to partially penetrate into the membrane and bind DAG. The molecular motion accompanying the membrane penetration would then remove the pseudosubstrate from the active site, leading to enzyme activation. The present study lends further credence to this model and explains how and why PKCγ is activated by a different mechanism. The C1A domain of PKCα has much higher DAG affinity than the C1B domain, and thus under physiological conditions only the C1A domain is expected to bind DAG. On the other hand, PKCγ has two C1 domains with comparable high DAG affinity and as a result it can bind two DAG molecules using both C1A and C1B domains. Furthermore, our activity and monolayer assays indicate that the two C1 domains of PKCγ are much less conformationally restricted than the C1A domain of PKCα and can readily penetrate the membrane and bind DAG in the membrane. Due to its relatively loose structure, the activation of PKCγ does not specifically require PS that was implicated in releasing the tethering of C1A domain of PKCα.

Differential membrane binding and activation mechanisms of the two conventional PKC isoforms are also evident in their cellular membrane translocation behaviors. When $[Ca^{2+}]_i$ was reduced to a basal level with BAPTA-AM, PKCα responds extremely slowly to DiC_8 addition because of conformational restriction of its C1A domain. Once the tethering of the C1A domain of PKCα is relieved by the D55A mutation, it can migrate to the plasma membrane much more rapidly in response to DiC_8. In agreement of its *in vitro* properties, PKCγ readily translocates to the plasma membrane, even faster than the D55A of PKCα under the same condition. Lack of effect by either D55A or D116A mutation on the membrane translocation of PKCγ also corroborates the notion that its C1A and C1B domains are not conformationally restricted as the C1A domain of PKCα. Although PKCγ exhibited lower activity than PKCα in the *in vitro* activity assay presumably due to the suboptimal selection of substrate for PKCγ, it is expected that PKCγ will show higher cellular activity than PKCα at submicromolar $[Ca^{2+}]_i$ owing to its much faster membrane translocation under these conditions.

Apparently, our cellular translocation data of PKCγ are at odds with the report by Oancea and Meyer (43), in which the C1 domains of PKCγ were proposed to be conformationally buried. This hypothetical model was based on the finding that the full-length PKCγ did not respond to PDBu or DiC_8 addition at basal $[Ca^{2+}]_i$, whereas its isolated C1B domain and C1A-C1B tandem construct readily translocated to the membrane under the same condition. It should be noted, however, the PDBu-induced membrane translocation of PKC is a poorly defined

process, because PDBu can be located at various cellular membranes as well as at the cytoplasm and at the nucleoplasm due to its low lipophilicity. We also found that the full-length PKCγ did not respond to PDBu addition at basal $[Ca^{2+}]_i$.[3] In the presence of a more lipophilic PMA, however, PKCγ consistently translocated to the plasma membrane much faster than PKCα. Furthermore, we found that it is critical to feed the cell with the high concentration of DiC_8 to observe the membrane translocation of PKCγ because of rapid breakdown of DiC_8 in the cell membrane. It is therefore possible that lack of DiC_8-induced membrane translocation of PKCγ reported by Oancea and Meyer (43) is due to the low concentration of DiC_8 used in the study.

In summary, this study demonstrates that two homologous conventional PKC isoforms, PKCα and PKCγ, have distinct membrane binding and activation mechanisms due to differences in DAG affinity and conformational flexibility of their C1 domains. As with other Ca^{2+}-sensitive conventional PKCs, PKCγ would be readily activated by DAG at the elevated $[Ca^{2+}]_i$. Even in the absence of a significant rise in $[Ca^{2+}]_i$, however, PKCγ with two readily accessible C1 domains can respond to the spatiotemporal dynamics of DAG turnover. PKCγ has been shown to be specifically localized in the brain and spinal cord and implicated in the modulation of synaptic plasticity (44). Further studies will reveal how these unique properties of PKCγ are coupled with its neuronal functions.

REFERENCES

1. Newton, A. C. (2001) *Chem. Rev.* **101,** 2353–2364
2. Newton, A. C. (2003) *Biochem. J.* **370,** 361–371
3. Zhang, G., Kazanietz, M. G., Blumberg, P. M., and Hurley, J. H. (1995) *Cell* **81,** 917–924
4. Ron, D., and Kazanietz, M. G. (1999) *FASEB J.* **13,** 1658–1676
5. Cho, W. (2001) *J. Biol. Chem.* **276,** 32407–32410
6. Kazanietz, M. G. (2002) *Mol. Pharmacol.* **61,** 759–767
7. Brose, N., and Rosenmund, C. (2002) *J. Cell Sci.* **115,** 4399–4411
8. Sutton, R. B., Davletov, B. A., Berghuis, A. M., Sudhof, T. C., and Sprang, S. R. (1995) *Cell* **80,** 929–938
9. Nalefski, E. A., and Falke, J. J. (1996) *Protein Sci.* **5,** 2375–2390
10. Rizo, J., and Sudhof, T. C. (1998) *J. Biol. Chem.* **273,** 15879–15882
11. Nishizuka, Y. (1988) *Nature* **334,** 661–665
12. Newton, A. C. (1995) *Curr. Biol.* **5,** 973–976
13. Slater, S. J., Kelly, M. B., Taddeo, F. J., Rubin, E., and Stubbs, C. D. (1994) *J. Biol. Chem.* **269,** 17160–17165
14. Slater, S. J., Ho, C., Kelly, M. B., Larkin, J. D., Taddeo, F. J., Yeager, M. D., and Stubbs, C. D. (1996) *J. Biol. Chem.* **271,** 4627–4631
15. Szallasi, Z., Boggi, K., Gohari, S., Biro, T., Acs, P., and Blumberg, P. M. (1996) *J. Biol. Chem.* **271,** 18299–18301
16. Bogi, K., Lorenzo, P. S., Szallasi, Z., Acs, P., Wagner, G. S., and Blumberg, P. M. (1998) *Cancer Res.* **58,** 1423–1428
17. Medkova, M., and Cho, W. (1999) *J. Biol. Chem.* **274,** 19852–19861
18. Bittova, L., Stahelin, R. V., and Cho, W. (2001) *J. Biol. Chem.* **276,** 4218–4226
19. Kashiwagi, K., Shirai, Y., Kuriyama, M., Sakai, N., and Saito, N. (2002) *J. Biol. Chem.* **277,** 18037–18045
20. Irie, K., Oie, K., Nakahara, A., Yanai, Y., Ohigashi, H., Wender, P. A., Fukuda, H., Onishi, H. K., and Kikkawa, U. (1998) *J. Am. Chem. Soc.* **120,** 9159–9167
21. Burns, D. J., and Bell, R. M. (1991) *J. Biol. Chem.* **266,** 18330–18338
22. Medkova, M., and Cho, W. (1998) *Biochemistry* **37,** 4892–4900
23. Bers, D. M. (1982) *Am. J. Physiol.* **242,** C404–C408
24. Stahelin, R. V., and Cho, W. (2001) *Biochemistry* **40,** 4672–4678
25. Bittova, L., Sumandea, M., and Cho, W. (1999) *J. Biol. Chem.* **274,** 9665–9672
26. Cho, W., Bittova, L., and Stahelin, R. V. (2001) *Anal. Biochem.* **296,** 153–161
27. Stahelin, R. V., Rafter, J. D., Das, S., and Cho, W. (2003) *J. Biol. Chem.* **278,** 12452–12460
28. Xu, R. X., Pawelczyk, T., Xia, T.-H., and Brown, S. C. (1997) *Biochemistry* **36,** 10709–10717
29. Cho, W., Digman, M., Ananthanarayanan, B., and Stahelin, R. V. (2003) *Methods Mol. Biol.* **233,** 291–298
30. Mozsolits, H., and Aguilar, M. I. (2002) *Biopolymers.* **66,** 3–18
31. Mozsolits, H., Thomas, W. G., and Aguilar, M. I. (2003) *J. Pept. Sci.* **9,** 77–89
32. Slater, S. J., Seiz, J. L., Cook, A. C., Buzas, C. J., Malinowski, S. A., Kershner, J. L., Stagliano, B. A., and Stubbs, C. D. (2002) *J. Biol. Chem.* **277,** 15277–15285
33. Kohout, S. C., Corbalan-Garcia, S., Torrecillas, A., Gomez-Fernandez, J. C., and Falke, J. J. (2002) *Biochemistry* **41,** 11411–11424
34. Marais, R. M., Nguyen, O., Woodgett, J. R., and Parker, P. J. (1990) *FEBS Lett.* **277,** 151–155
35. Geiges, D., Meyer, T., Marte, B., Vanek, M., Weissgerber, G., Stabel, S., Pfeilschifter, J., Fabbro, D., and Huwiler, A. (1997) *Biochem. Pharmacol.* **53,** 865–875
36. Verger, R., and Pattus, F. (1982) *Chem. Phys. Lipids* **30,** 189–227
37. Bazzi, M. D., and Nelsestuen, G. L. (1988) *Biochemistry* **27,** 6776–6783
38. Souvignet, C., Pelosin, J. M., Daniel, S., Chambaz, E. M., Ransac, S., and Verger, R. (1991) *J. Biol. Chem.* **266,** 40–44
39. Blume, A. (1979) *Biochim. Biophys. Acta* **557,** 32–44
40. Demel, R. A., Geurts van Kessel, W. S. M., Zwaal, R. F. A., Roelofsen, B., and van Deenen, L. L. M. (1975) *Biochim. Biophys. Acta* **406,** 97–107
41. Marsh, D. (1996) *Biochim. Biophys. Acta* **1286,** 183–223
42. Slater, S. J., Kelly, M. B., Taddeo, F. J., Ho, C., Rubin, E., and Stubbs, C. D. (1994) *J. Biol. Chem.* **269,** 4866–4871
43. Oancea, E., and Meyer, T. (1998) *Cell* **95,** 307–318
44. Saito, N., and Shirai, Y. (2002) *J Biochem.* (*Tokyo*) **132,** 683–687

[3] R. V. Stahelin and W. Cho, unpublished observation.